CrossMark

ORIGINAL PAPER

Experimental Investigations on Building Derived Materials in Chemically Aggressive Environment as a Partial Replacement of Soil in Geotechnical Applications

Ashok Kumar Suluguru · Shreyans R. Surana · Anasua GuhaRay · Arkamitra Kar · Jayatheja Muktinutalapati

Abstract Construction and associated demolition processes produce huge amount of solid waste, generally termed as construction and demolition waste (CDW). Management and proper disposal of these wastes is an area of prime concern for modern civil engineers. About 90% of all CDW is composed of building derived materials (BDM) obtained from concrete, bricks, and tiles from structural and non-structural elements of a building. The present study emphasizes on the use of virgin BDM, which conserves natural aggregate, reduces the impact on landfills, saves energy, and thus can provide significant cost benefit. Five types of BDM—crushed lightweight concrete (T1), crushed marble tiles (T2), crushed high strength concrete (T3), crushed normal portland cement concrete (T4), and crushed bricks (T5)—are characterised to assess their compatibility when used in conjunction with local soil. The soil, BDM and soil–BDM mixes are characterized from physical, mechanical, mineralogical, microstructural, and chemical aspects. These tests are then repeated for the aforementioned soil-BDM mixes after immersion in acids. Aggregate impact value (AIV) results on the five types of BDM indicate that T1 and T5 are poorly resistant to impact loads. However, T2, T3, and T4 show relatively better resistance to impact loads and satisfy the requirements for sub-base material standards. Shear strength studies show that the average optimum replacement of soil by BDM is in the range of 17–23% by mass. In order to test the compatibility of BDM in soils containing aggressive chemicals, the properties mentioned above are re-evaluated after exposing the BDM to aggressive chemical environments. The results indicate that the internal angle of friction (ϕ) of virgin BDM is found to vary significantly due to acid attack. The results of AIV after exposing the BDM to acids show that BDM are highly susceptible to chemically aggressive environment. The performance of all types BDM are affected by the presence of acids and appropriate measures must be adopted while using BDM in such chemically aggressive environment. These standards can be used as guidelines in the present study in the absence of specific standards for BDM applications.

Electronic supplementary material The online version of this article (https://doi.org/10.1007/s10706-018-0662-0) contains supplementary material, which is available to authorized users.

A. K. Suluguru · S. R. Surana · A. GuhaRay (✉) ·
A. Kar · J. Muktinutalapati
Civil Engineering Department, BITS-Pilani Hyderabad,
Secunderabad 500078, India
e-mail: guharay@hyderabad.bits-pilani.ac.in

1 Introduction

In the modern era, rapid urbanisation and development of infrastructure in a developing country like India leads to production of huge construction and demolition wastes (CDWs). The periodic modification and renovations of new and existing structures like bridges and flyovers also contribute to the accumulation of CDW. Moreover, natural calamities like earthquakes add to the generation of these wastes. The United States Environmental Protection Agency (USEPA) defines CDW as waste materials consisting of the debris generated during the construction, renovation, and demolition of buildings, roads, and bridges (USEPA 2017). As the construction industry greatly contributes to the present environmental unbalances, it is necessary to (1) drastically reduce the consumption of non-renewable natural resources; and (2) limit the dumping of rejected BDM that consumes gradually diminishing space. Transporting the CDW from the site of generation and their disposal into dumping yards incur additional expenses and hazard to the environment. Hence there is need for recycle and reuse of these CDW in an innovative manner. The primary component of CDW is building derived materials (BDM), consisting of concrete, brick, tiles, wood, and plastic (Bhattacharyya et al. 2013).

Several researchers have investigated the use of different kind of C&D waste materials in varied engineering applications due to the shortage of natural aggregates and to arrive at an economic alternative (Meyer 2004). Recycling of BDM incurs extra cost due to chemical and mechanical refinement processes associated with it. Hence, there are practical difficulties associated with establishing waste management and recycling plants (Sustainability Victoria 2005; Arulrajah et al. 2012; Poon and Chan 2006). The state of Delhi in India alone generated 1.5 million tons of debris from 2009 to 2014. But till date, there are only three existing waste recycling facilities available in India as per the report in The Hindu (2017). Debieb and Kenai (2008) experimentally observed that the resilient modulus of loose soils and soft deposits increased proportionally with addition of CDW McKelvey et al. (2002) studied the shear parameters and strength behavior of recycled concrete aggregate (RCA) using large shear box (300 mm × 300 mm × 200 mm) and reported that the value of angle of internal friction is about 39°. Rathje et al. (2006)

conducted large direct shear box and triaxial tests on RCA and reported a cohesion value of 62 kPa and angle of internal friction of 46°. Arulrajah et al. (2011) studied the geotechnical properties of recycled crushed brick and suggested to blend it with some other recycled materials to study its performance in geotechnical applications. Researchers such as Sobhan and Krizek (1998), Tam and Tam (2007) and Courard et al. (2010) discussed the geotechnical properties of recycled concrete aggregates in various geotechnical applications and reported that RCA can be used in pavement applications successfully. Hasan et al. (2016) evaluated the effect of recycled aggregates on soil stabilization and observed that the shear properties of soil are improved on stabilizing with recycled aggregates. Cardoso et al. (2013) conducted tests to improve the geotechnical properties of soil and observed an increase in maximum dry density (MDD) and optimum moisture content (OMC) values. Similarly, Taha et al. (2002) and Hoyos et al. (2011) studied the geotechnical characteristics of reclaimed asphalt pavement and reported that stabilization of reclaimed asphalt pavement with cement enhanced the strength and stiffness characteristics for using them as sub base material in pavement applications. In existing practice, BDM are used in the form of recycled coarse aggregates. The application of recycled aggregates has started in several Asian and western countries for construction projects (Rao et al. 2007). Recycled aggregates have previously been used in limited quantities to enhance the performance of pavements, with the goal of using BDM in near future (Melton 2015). However, no systematic study has been reported regarding their physical and chemical characterizations. Moreover, limited studies have been reported about their utilization for ground improvement. This study thus aims to evaluate the utility of BDMs in ground improvement, which, in turn, will reduce the dumping of these BDM into landfills. Behaviour of BDM in the soil will depend upon the type of soil and the contaminants present in the soil. Acids like sulphate and chloride are well known for their detrimental effect on concrete (Zuquan et al. 2007). If the soil is near industrial or agricultural area, it may contain nitrate as well. Due to rapid urbanization, these sites, which were once considered marginal, are now being extensively considered for infrastructure development. Thus, to use BDM in such soil, the present study characterizes them through

physical investigations, microscopy, and exposure to chemically aggressive environment like sulphate, chloride, and nitrate to study their response.

The present study is conducted at the Hyderabad campus of the Birla Institute of Technology and Science (BITS)-Pilani. The campus is undergoing renovation and expansion and consequently, generating large quantities of BDM. Crushed lightweight concrete (T1), crushed marble tiles (T2), crushed high strength concrete (T3), crushed normal Portland cement concrete (T4), and crushed bricks (T5) are collected and evaluated for ground improvement. The microstructural, physical, mechanical, and chemical characteristics of these BDMs are studied to assess its potential for ground improvement. The results obtained from specific gravity test, water absorption test and AIV test on BDM are compared with standard results for natural aggregates, owing to the lack of available data for any kind of BDM. X-ray diffraction (XRD) studies and microanalyses through scanning electron microscopy (SEM) and energy dispersive X-ray spectroscopy (EDS) are conducted to identify the chemical composition of the five kinds of BDM and the soil–BDM mixes. Shear strength characteristics are evaluated for different soil–BDM combinations to identify the optimum BDM content for partial replacement of soil. In the second stage, all types of BDM are immersed in solutions of sulfuric acid (5% v/v), nitric acid (5% v/v), and hydrochloric acid (5% v/v) for 7 days. The tests are repeated on BDM after exposure to these acids to identify their effect on the performance of the BDM. According to ASCE, there are no global standards for any kind of virgin BDM in geotechnical applications at present (Melton 2015; Edil 2015). Hence, the results obtained from the present study can be used to establish a basis for the practical use of BDM and provide recommendations to prepare standard codes of practice for these materials. The next section presents the details of the materials and experimental methods used in this study.

2 Materials and Experimental Methodology

2.1 Materials Used

2.1.1 Soil

Locally available river sand, collected from the banks of river Krishna from the state of Telangana of India is used for the present study. The soil is classified as SP according to unified soil classification system (USCS). The engineering properties of soil are presented in Table 1.

BDM is collected from local construction and demolition activities at the Hyderabad campus of BITS-Pilani in Telangana, India (Fig. 1). Based on suggestions from existing literature for the inclusion of foreign materials in soil, the procured BDM is crushed to the sizes less than 10 mm (Lee et al. 1999).

2.1.2 Acids

Commercially available laboratory grades of sulfuric acid, hydrochloric acid, and nitric acid are procured, and necessary amounts of de-ionized water are added to prepare the respective 5% v/v solutions. The experimental techniques are detailed in the following section.

2.2 Experimental Methodology

2.2.1 Mineralogical Characterization

X-ray diffraction (XRD) is used to identify the minerals present in the BDM through a Bruker D8

Table 1 Engineering properties of soil

Properties	Values
Specific gravity, G	2.60
Coefficient of uniformity (C_u)	2.5
Coefficient of curvature (C_c)	0.9
Maximum dry density, γ_{max} (gm/cc)	1.928
Minimum dry density, γ_{min} (gm/cc)	1.662
Maximum void ratio, e_{max}	0.636
Maximum void ratio, e_{min}	0.411
USCS classification	SP
Internal angle of friction, ϕ (°)	28°

(i) Light Weight Concrete BDM(T1)   (ii) Marble BDM(T2)   (iii) High strength concrete BDM(T3)

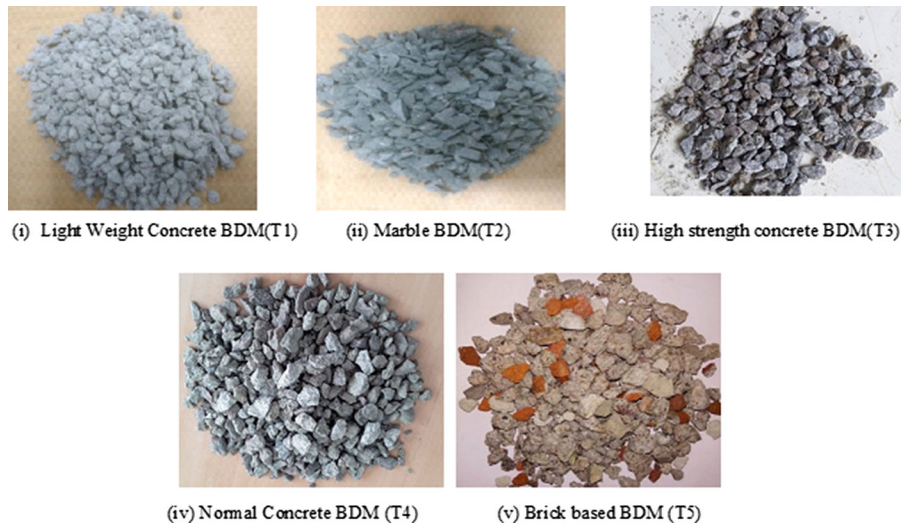(iv) Normal Concrete BDM (T4)   (v) Brick based BDM (T5)

Fig. 1 Types of building derived materials

Discover setup. CuKα X-rays are generated at 40 mA and 40 kV. Scans are performed over 0–100° 2θ range at 0.02° 2θ steps and integrated at the rate of 2 s per step. Mineralogical characterization is crucial for assessing the compatibility of the different types of BDM to be used in conjunction with soil in geotechnical applications.

2.2.2 Microstructural Characterization Through SEM–EDS

Scanning electron microscopy (SEM) aims to plot high-resolution micrographs to characterize the surface morphology of the soil and the BDM. EDS analysis is useful in identifying the elements and contaminants as well as estimating their elemental composition. Knowledge of the chemical compositions of the soil and the BDM is necessary to identify their compatibility when used in combination in practical applications. The microstructural analyses are conducted using a JEOL Ltd. JSM 7600-F field emission scanning electron microscopy (FE-SEM), equipped with an energy dispersive X-ray spectroscopy (EDS) analyzer. The images are captured at magnifications of 50×, 2000×, and 5000×. For each type of soil–BDM combination, three regions are located at random for capturing the images due to the uncertainty and inherent lack of homogeneity of the microstructure of these materials. The operating voltage is 10 kV. The working distance is maintained

between 8 and 15 mm and the probe current at 65.4–67.0 μA in order for the EDS analyzer to work properly. Before the SEM-EDS analyses, the BDM are oven-dried at 105 °C for 24 h in order to get rid of any internal moisture. Then, they are coated with a 15 nm layer of platinum in argon gas atmosphere at vacuum, in order to make them electrically conductive in nature.

2.2.3 Physical Characterization

Stereo microscopic imaging is carried out to identify the particle size distribution and superficial physical features of the BDM using an Olympus SXZ7 setup. It is used to investigate the dimensions of the different particles comprising the crushed BDM having maximum size of 10 mm. The images were captured at the magnification of 3.2 × . Dimensions of the region of interest in Fig. 4 are 3.376 mm × 1.894 mm. The minimum dimension that can be identified by this microscope is 20 μm. Stereo microscopy is also used to identify the changes in these surface features of the BDM after their immersion in the different acids and to study the effect of these deposited salts on the performance of the BDM when get mixed with soil undergoing various geotechnical tests. Identification of the respective gradations of soil and BDM is necessary to evaluate the effects on compaction characteristics due to the addition of BDM to soil.

2.2.4 Mechanical Characterization

The five different types of BDM are crushed to a maximum size of 10 mm. Grain size analysis is carried out for soil, BDM, and for soil with different proportions (0, 5, 10, 20, and 30%) of BDM to study the uniformity and compatibility in the sizes of both soil and BDM, according to the IS: 2720-Part 4 (1985) and ASTM D6913/D6913M-17 (2017).

Specific gravity and aggregate water absorption of BDM (maximum size of 10 mm) are also determined to evaluate their compatibility with soil according to the IS 2386–3 (2011), ASTM D854-06e1 (2016) and ASTM C127-15 (2016) respectively.

For impact value test, materials sieved through 12.5 mm and retained on 10 mm are used as test material. Aggregate impact value (AIV) test is conducted according to the IS 2386-Part 4 (2011) and ASTM C131/C131M-14 (2006) to find the resistances of BDM to degradation under impact loading. Materials sieved through 12.5 mm and retained on 10 mm are used as test material. Similarly, the AIV test conducted to determine the effect of acids on materials after immersion for 7 days.

Large shear box test is conducted as per the guidelines of IS 2720-Part 39 (1979) and ASTM D3080/D3080M-11 (2011) to determine the internal angle of friction of different types of BDM. A large-scale direct shear test apparatus measuring 300 mm in length, 300 mm in width and 200 mm in depth is used to determine the shear strength of the BDM. Following IS 2720-Part 39 (1979), the maximum size of particles which can be tested in a shear box is 1/10 of the maximum dimension of the box. Hence the dimension of the box is chosen as 300 mm × 300 mm, in which the maximum dimension of particle which can be tested is 30 mm. However, this test considers the failure plane to be horizontal, which is not always true. The tests are conducted on soil replaced with 0–30% BDM. The testing apparatus has two boxes: a fixed upper box and a moveable lower box. Initially, the lower and upper boxes are clamped while preparing the samples for the tests. The samples are compacted in the shear box in three layers by using hand tamping with a plastic hammer to attain maximum dry density obtained from the vibratory table method. The shearing stage of the test is conducted under three normal stress levels of 1.25, 1.75 and 2.25 kg/cm^2. A shear displacement rate of 0.028 mm/min is maintained throughout the shearing stage. The tests were terminated once the horizontal shear displacement reaches approximately 75 mm.

2.2.5 Response to Acid Attack

As mentioned earlier, soil may contain different sulfates, chlorides, and nitrates depending on its location. In order to simulate the field conditions in the laboratory, the BDM samples are tested after separate immersions in sulfuric acid, hydrochloric acid, and nitric acid for 7 days. 5% v/v solutions of sulfuric acid, hydrochloric acid and nitric acid are prepared for testing the sulfate, chloride and nitrate attacks respectively. The BDM samples are crushed to the required size and transported to the laboratory and immersed in three different acids for 7 days. The acids mentioned above are taken in volume of 5% and prepared solution with replacing the 5% of distilled water in l000 ml, which makes the 5% v/v solution. The BDM, thus immersed in acids is taken out and air dried for one hour. After this, the air-dried BDM are collected in iron bowls and oven dried at 105 °C for 24 h in order to get rid of moisture in the immersed BDM. The BDM later used in measured quantities to carry out all the above mentioned tests. Each of the tests mentioned in Sect. 2.2.1–2.2.4 are conducted on the different types of BDM and soil-BDM mixtures before and after their immersion in the three separate acid solutions. The results from these tests before acid attack are compared with those after acid attack to evaluate the acid-resistance of the different types of BDM. The following section describes the results and discussions from each of the above experiments.

3 Results and Discussions

This section presents the results obtained from each experiment along with the corresponding observations and discussions based on those experiments.

3.1 Mineralogical Characterization Through X-ray Diffraction (XRD)

The X-ray diffraction patterns for powdered BDM are shown in Fig. 2. For T1 in Fig. 2i, the prominent sharp peaks at 2θ values of 26.24° and 26.80° represent crystalline quartz (Q). The smaller peaks between 2θ
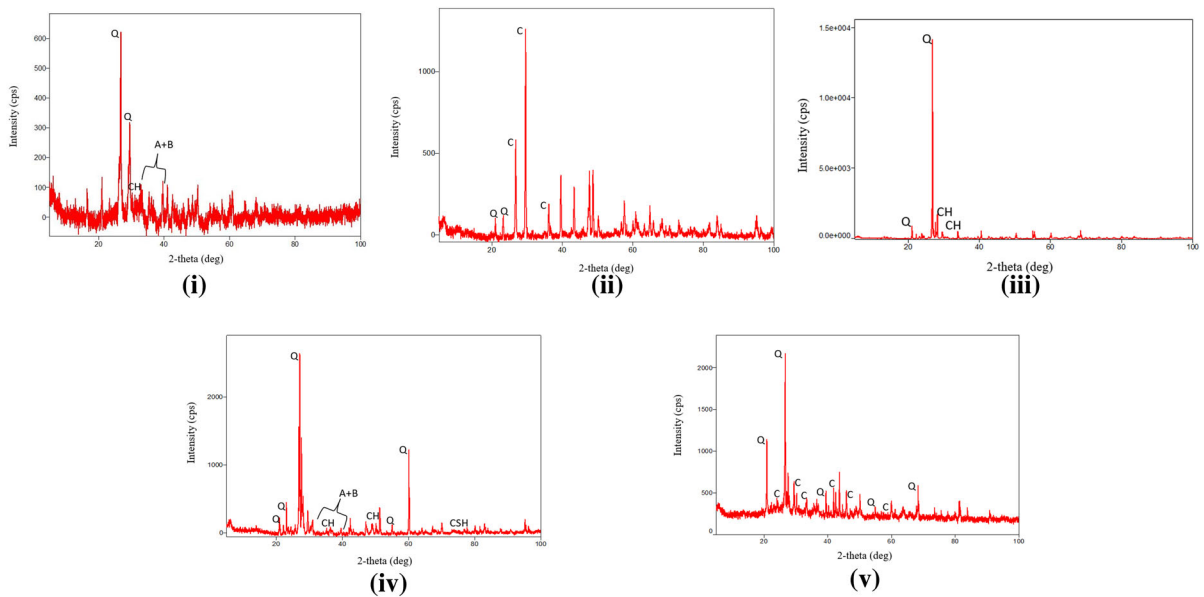
Fig. 2 Powder X-ray diffractograms for **i** T1, **ii** T2, **iii** T3, **iv** T4 and **v** T5

values of 30° to 40° represent the tricalcium silicate or alite (A), and dicalcium silicate or belite (B) component of Portland cement. The peak near the 2θ value of 34° represents calcium hydroxide (CH) or portlandite component due to hydration of Portland cement. For T2 in Fig. 2ii, the prominent peaks at 2θ values of 23.20° and 26.76° represent crystalline quartz. The sharp peaks at 2θ values of 29.59°, 36.14°, and 36.70° represent calcite (C). For T3 in Fig. 2iii, the sharp peaks at 2θ values of 21.03°, 23.18°, and 29.22° represent the quartz (Q). The smaller peaks at 2θ values of 31.10°, 33.96°, and 36.72° are attributed to the calcium hydroxide (CH) component due to hydration of Portland cement. For T4 in Fig. 2iv, the sharp peaks corresponding to 2θ values near 20.96°, 22.12°, and 28.41°, 55°, and 60° represent crystalline quartz (Q). The smaller peaks between 2θ values of 30–40° represent the tricalcium silicate or alite (A) and dicalcium silicate or belite (B) component of Portland cement. The peaks near 2θ values of 16°, 34° and 49° represent the calcium hydroxide (CH) or portlandite component due to hydration of Portland cement. The flatter portions of the diffractogram represented by small humps indicate the presence of amorphous hydrated cementitious paste component (calcium silicate hydrate, CSH). These conclusions are drawn after comparing with existing literature (Kupwade and Allouche 2011; Kar et al. 2014; Mindess et al. 2003).

For T5 in Fig. 2v, the peaks reveal the predominance of crystalline quartz (Q) and calcite (C) as expected for bricks (EI Gohary and AI Naddaf 2009). The sharp peaks corresponding to 2θ values near 21°, 26°, 39°, 55°, and 66° represent crystalline quartz (Q). The sharp peaks corresponding to 2θ values near 26°, 30°, 36°, 45°, 47°, and 59° represent calcite (C) (EI Gohary and AI Naddaf 2009; Fang et al. 2015).

As mentioned earlier XRD provides only qualitative results. Hence, SEM and EDS are used in conjunction for quantitative characterization of the materials, as presented in the following section.

3.2 Microstructural Characterization Through SEM-EDS

Figure 3 presents SEM micrographs and corresponding EDS analyses for soil + T1. Although SEM-EDS analyses are performed for soil with different percentages of all five types of BDM, the images for only soil + 20% T1 are presented here for the sake of brevity. The remaining images are provided as supplementary information (Fig. S.3.1 to S.3.4). Soil is found to be composed mainly of O and Si, as expected in sand. Some Al and Fe are also detected along with trace amount of Ca. These results are in agreement with the findings from existing literature (Taylor 1997; Sadrekarimi and Olson 2009). The
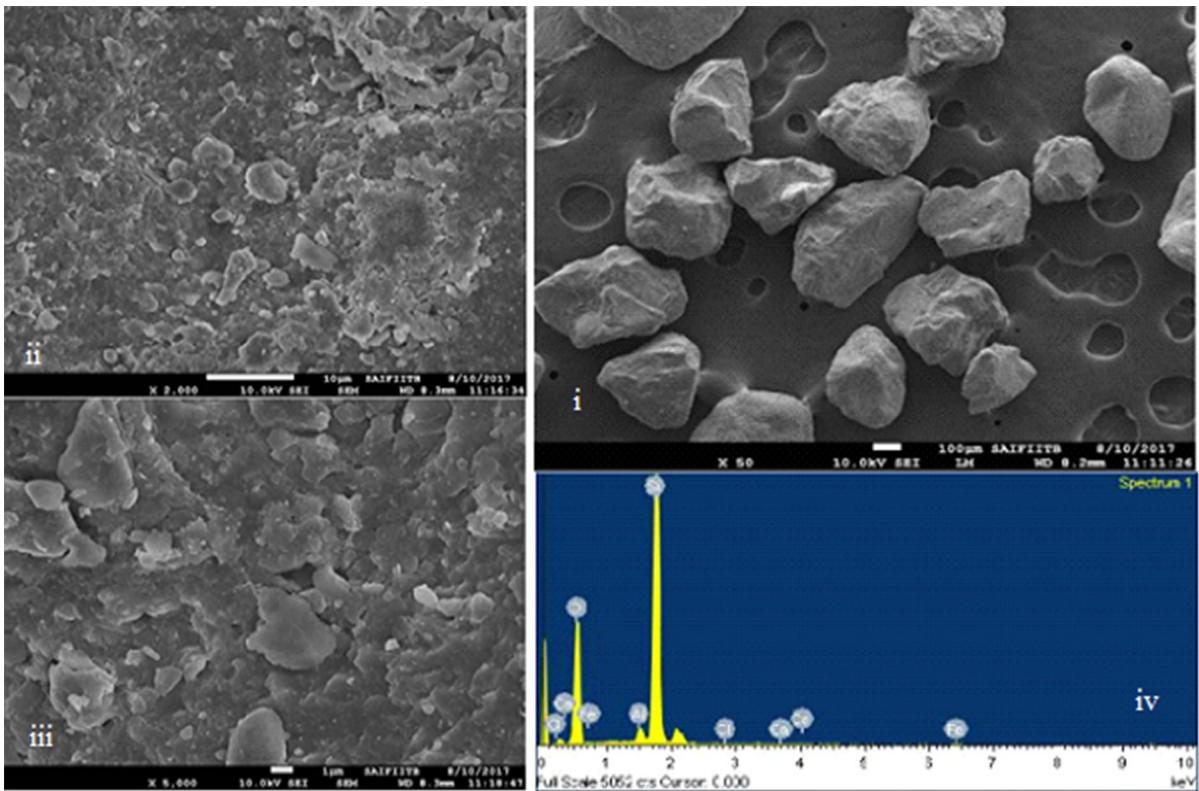
Fig. 3 SEM and EDS images for soil + 20% T1

detailed micrographs are provided in a separate study by the present authors (Suluguru et al. 2017).

When the whole area shown in Fig. 3i is scanned by the EDS setup, a combined elemental analysis for the soil + 20% T1 is obtained (Table 2). Since T1 is generated by the demolition of lightweight concrete, increase in the relative Ca content is observed when it is added to the soil (Table 2).

The micrographs for soil + 20% T2 (Fig. S.3.1) reveal a relatively uniform and more homogeneous compared to the other types of BDM. This is due to the polished surface of the tiles and marbles which led to the generation of T2. Elemental composition for soil + 20% T2 (Table S.2.1) showed the presence of Si, Al, and Ca as expected in case of BDM originating from calcite-rich sources. The elemental composition for soil + 20% T3 shows the presence of Si, Al, Ca and Fe (Table S.2.2). Soil + 20% T4 showed the presence of Si, Al and Fe (Fig. S.3.3). The elemental composition for soil + 20% T4 is shown in Table S.2.3. The presence of Si, Al, Fe and small amount of chloride (Cl) is observed in soil + 20% T5

Table 2 EDS elemental analysis for soil + 20% T1

Element	Weight%	Atomic%
O K	50.77	64.84
Al K	1.68	1.27
Si K	45.51	33.11
Cl K	0.00	0.00
Ca K	0.23	0.12
Fe K	1.81	0.66

showed (Fig. S.3.4) may be because of impurities present in T5. The elemental composition for soil + 20% T5 is shown in Table S.2.4.

3.3 Physical Characterization Through Stereomicroscopy

The virgin BDM particles having a maximum size of 10 mm are investigated under the stereomicroscope. The images for five types of BDM are presented in Fig. 4. The regions of interest are selected at random.
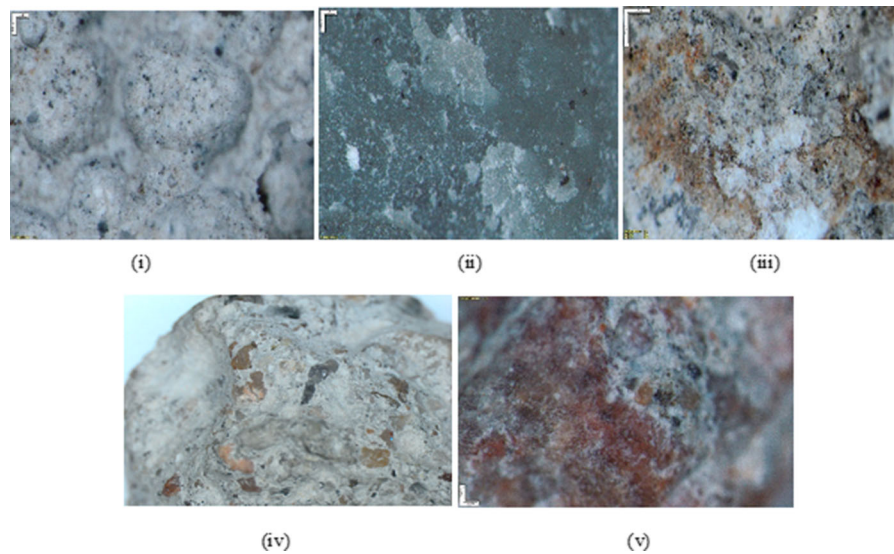
Fig. 4 Stereo microscopic image at 3.2 × magnification for BDM particle **i** T1, **ii** T2, **iii** T3, **iv** T4 and **v** T5

Visual inspection for T1(Fig. 4i) shows a greyish portion which indicates the hardened cementitious component and it clearly shows voids present in it as it is porous concrete material. For T2 (Fig. 4ii), a generally uniform pattern is visible on the surface as it made up of predominantly one kind of material. The visual inspection for virgin T3 (Fig. 4iii) shows the presence of hardened cementitious paste, cement-mortar, and aggregates. Visual inspection of the images shows that virgin T4 (Fig. 4iv) consists of hardened cementitious paste, cement-mortar, and aggregates whereas greyish areas on the image indicate the hardened cementitious and cement mortar. The brownish regions indicate soil particles and the blackish areas are most likely to indicate the limestone aggregate components. Visual inspection of the image for virgin T5 (Fig. 4v) shows the presence of fire-red colored clay-brick portion and the greyish mortar portion.

3.4 Mechanical Characterization

3.4.1 Grain Size Analysis

Gradation analysis is carried out for soil, virgin BDM and soil-BDM blends. Figure 5 shows the particle size distribution curves for soil and five types of BDM. From Fig. 5, it can be observed that the values of the shape parameters, coefficient of uniformity (C_u) and

coefficient of curvature (C_c) of soil are reported as 2.5 and 0.9 respectively, which shows that it is a poorly graded material. T5 is classified as GW and the other types (T1–T4) are classified as GP according to unified soil classification system (USCS). The C_u and C_c of T1 are found to be 1.45 and 0.95 respectively. The gravel (> 4.75 mm), soil (0.075–4.75 mm) and silt and clay (< 0.075 mm) sized particles present in T1 are found to be 91.08, 8.63 and 0.29% respectively. The values of C_u and C_c of a typical heavyweight material are 78.83 and 2.97 respectively (Rahman et al. 2014a, b). Also, for a typical lightweight material, the gravel, soil and silt and clay fractions are less than 40, 70 and 3% respectively (Harmon 2014; Misapor 2014), while that of heavyweight material is 47.9, 42.2 and 9.9% respectively. From the analysis, T1 can be classified as a heavyweight material. Accordingly, from the results T2, T3, T4 and T5 are also reported as heavy weight materials. Particle size distribution curves for all soil–BDM blends in varying percentages by weight of BDM are presented in supplementary data (Fig S.5.1). It is seen that the values of the shape factors, C_u and C_c vary proportionally with the T1 content in soil (Tables 3 and 4). The gradation of soil thus improves upon addition of T1. Similarly, it is observed from the grain size analysis that the C_u and C_c of soil improved upon addition of T2, T3, T4 and T5 (Fig. S.5.1.a–S.5.1.d and Table S.4.1–S.4.4).
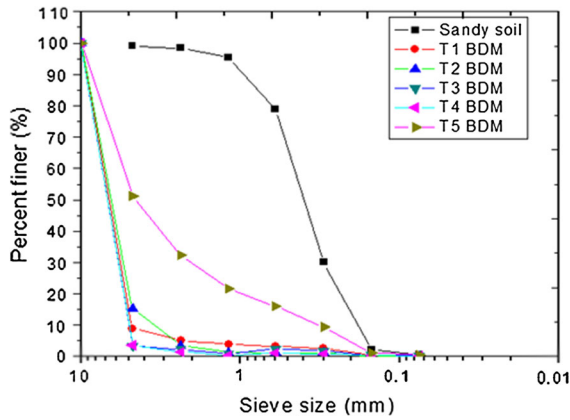
Fig. 5 Grain size analysis of soil and five types of BDM

Table 3 Values of shape factors of BDM

Type of BDM	C_u	C_c
T1	1.45	0.95
T2	2.09	1.14
T3	1.44	1.01
T4	1.43	0.99
T5	15.2	2.27

Table 4 Values of shape factors of soil at different proportions of T1

Soil + T1	C_u	C_c
Soil	2.5	0.9
T1	1.45	0.95
5% T1	1.66	0.97
10% T1	2.11	0.98
20% T1	2.13	1.01
30% T1	2.72	1.05

3.4.2 Specific Gravity and Water Absorption

The average specific gravity results for five types of BDM are provided in Table 5. The values of specific gravity of aggregates used in cement concrete applications lie between of 2.5 and 3.0. The specific gravity value of T1 is 1.23. The reason for such a low value can be attributed to the fact that it is a light weight material and hence it is not within the permissible limits as per IS 2386-3 (2011). The average results of specific gravity for T2, T3, T4 and T5 used for the present study are within the limits and thus almost

Table 5 Specific gravity value for all BDM

Type of BDM	Specific gravity value	Water absorption value
T1	1.23	23.53
T2	2.72	2.33
T3	2.43	6
T4	2.54	1.18
T5	2.43	3.28

complying with the permissible value of the standard values for coarse aggregates can be used for partial replacement in soil.

The average water absorption results (from three tests) for T4 is 1.182%, which is less than the maximum permissible limit of 2% for aggregates used in cement concrete applications. The average water absorption results for T1, T2, T3 and T5 are more than the permissible value tabulated in Table 5. These two tests serve as a metric to evaluate the quality of BDM obtained from various sources. In the absence of standard values for any kind of BDM, comparisons are made with the existing parameters for coarse aggregates for cement concrete applications.

3.4.3 AIV Test

The AIV test is widely used in characterizing the capacity of materials to carry impact loads. The average AIV tests results for each type of BDM are presented in Table 6. The highest percent value indicates greatest extent of breakage during the test. The AIV results show that the particles tested (10 mm in size) of T1 are weakest and particles of T2, T3, T4 and T5 are strongest one to withstand the impact loads. AI value of T2 is within limits of IS 2386-Part 4 (2011) used for road surfacing in satisfactory manner. T3 shows AIV of 33.35% which is within the IS 2386-Part 4 (2011) restriction of 35% for aggregates used in cement concrete applications, as expected for high strength concrete which has higher capacity to resist impact loads. T4 and T5 have AIVs beyond the permissible limit for use in road surfacing. These results are in agreement with the findings from a previous study by the present authors (Suluguru et al. 2017). Concrete and brick undergo loss of load bearing capacity as age increases and the observations corroborate that effect. Hence, the user needs to be judicious regarding their reuse in practical scenarios.

Table 6 Aggregate impact value for all BDM

Type of BDM	Aggregate impact value (%)
T1	79
T2	27.53
T3	33.35
T4	37.76
T5	41.1

3.4.4 Large Shear Box Test

Large shear box test is conducted to find out the angle of internal friction of soil and soil-BDM blend. The schematic of large shear box is shown in Fig. 6 (Christopher et al. 2008). The friction angle (φ) for soil is found to be 28°. Results from this test are tabulated in supplementary data table in Table S.6. The results indicate that when BDM is added to soil, the interface friction angle increases proportionally, and it gives a positive indication to use BDM as partial replacement in soil. For T1, the value friction angle (φ) is quite high for 5% replacement in soil and showing least for 30% replacement of soil with T1. Similarly, for all types of BDM, the internal angle of friction (φ) is increased and the shear strength properties of soil are improved upon blending with BDM. The possible reason for the increase in φ value may be due to compatibility of soil and BDM

concluded from the sieve analysis results. Also it is clearly observed that, the average optimum content that to be added to soil to get improved internal angle of friction (φ) is approximately in the range of 17–23% for all types of BDM.

3.5 Response to Acid Attack

The following section presents the results obtained by replicating the above tests on the same soil + BDM blends after immersing them in separate 5% v/v solutions of HCl, H_2SO_4, and HNO_3.

3.5.1 XRD for BDM After Immersion in Acids for 7 Days

On comparison with Fig. 2i, immersion of T1 in hydrochloric acid for 7 days shows additional peaks (Fig. 7i) corresponding to $CaCl_2$ at 29°, 43°, 61°

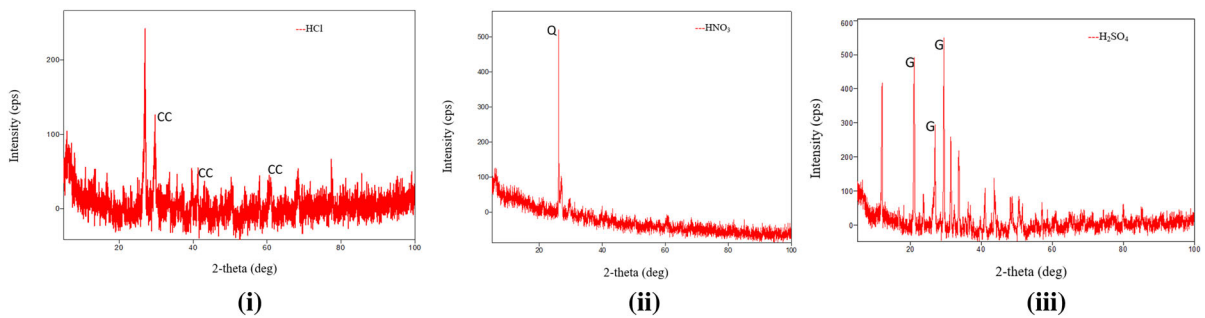**Fig. 6** Schematic of large-scale direct shear machine
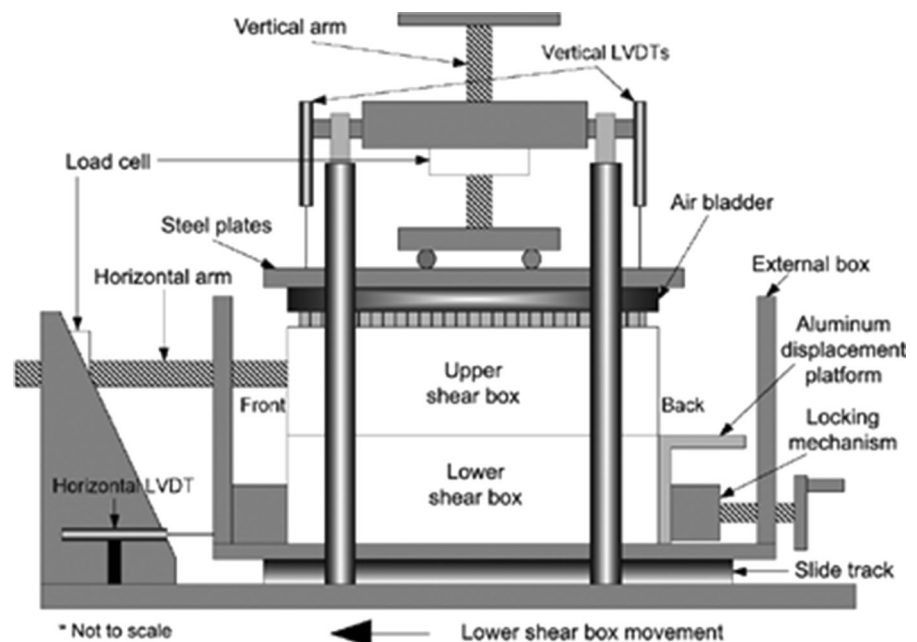
Fig. 7 X-ray diffractogram for T1 after 7 days of immersion in **i** hydrochloric acid (5% v/v) solution, **ii** nitric acid (5% v/v) solution, and **iii** sulfuric acid (5%v/v) solution

(Bontempi et al. 2010; Lim et al. 2010). This explains the surface deposition of $CaCl_2$ on the surface of T1 as visible through stereo microscope and the possible reason for the decrease in AIV and change in weight. T1 immersed in Nitric acid shows the peaks for quartz only at a 2θ value of 27.08° (Fig. 7ii). Almost all the peaks other than that of quartz which are visible in Fig. 2i, have become absent. This indicates the disintegration of the bonds present in concrete due to the acid attack. Sulfuric acid immersion results in additional peaks for gypsum, CaSO4.0.5H2O (G) at 2θ values near 21°, 23°, 29° (Fig. 7iii; U.S. Geological Survey 2016). This is expected due to the high sulfate content in sulfuric acid. This explains the change in appearance of the T1 when investigated through stereo microscope and the possible reason for the change in AIV. Remaining XRD results for all types of BDM are presented in supplementary data.

On examination and comparison with Fig. 2ii, T2 immersion in hydrochloric acid shows additional peaks for $CaCl_2$ at 2θ values near 29°, 31°, 43°, 61° (Fig. S.7.1.i; Bontempi et al. 2010; Lim et al. 2010; U.S. Geological Survey 2016). This explains the precipitation of $CaCl_2$ on the surface of T2 noticeable through stereo microscope. Similarly, T2 immersed in Nitric acid shows the peaks for calcium nitrate (CN) at 2θ values of 26.82° and 26.62° (Yildirim et al. 2015; Fig. S.7.1.ii). Sulfuric acid immersion of T2 resulted in additional peaks for gypsum, CaSO4.0.5H2O (G) at 2θ values of 20.76°, 23.12°, 29.14° (Fig. S.7.1.iii; U.S. Geological Survey 2016).

For T3 immersed in hydrochloric acid the additional peaks for $CaCl_2$ were observed at 2θ value of 29°, 31°, 42°, 43°, 61° (Fig. S.7.2.i; Bontempi et al. 2010; Lim et al. 2010). Peaks for KCl are also observed at 2θ values near 26°, 68°, 74° (Bontempi

et al. 2010; Lim et al. 2010). Similarly, T3 immersed in nitric acid shows the peaks for potassium nitrate (KN) at 2θ values near 26.82°, 28.62° and 67.85° (Fig. S.7.2.ii; Yildirim et al. 2015). On comparison with Fig. 2iii, Sulfuric acid immersion of T3 results in additional peaks for gypsum, CaSO4.0.5H2O (G) at 2θ values of 20.98°, 23.64°, 29.30° (Fig. S.7.2.iii; U.S. Geological Survey 2016).

When compared with Fig. 2iv, T4 immersion in hydrochloric acid shows, the additional peaks for $CaCl_2$ at 2θ values near 29°, 42° and 61° (Fig. S.7.3.i; Bontempi et al. 2010; Lim et al. 2010; U.S. Geological Survey 2016). Presence of KCl was also observed at 2θ values near 26°, 68°, 74.1°. For T4 immersed in nitric acid, additional peaks are observed for potassium nitrate, KNO_3 at 2θ values near 27°, 28° and 68° (Fig. S.7.3.ii; Yildirim et al. 2015). Similarly, additional peaks for gypsum, CaSO4.0.5H2O (G) at 2θ values near 21.38°, 23.2°, 29° (Fig. S.7.3.iii; U.S. Geological Survey 2016) for T4 immersed in sulfuric acid.

On comparison with Fig. 2v, T5 immersion in hydrochloric shows additional peaks for $CaCl_2$ at 2θ values near 42° and 61° (Fig. S.7.4.i; Bontempi et al. 2010; Lim et al. 2010; U.S. Geological Survey 2016). Peaks due to the presence of KCl are also observed at 2θ values of 26°, 28°, 68°. T5 immersed in nitric acid shows the peaks for potassium nitrate (KN) at 2θ values near 27°, 29°, and 68° (Fig. S.7.4.ii; Yildirim et al. 2015). Sulfuric acid immersion results in additional peaks for gypsum, CaSO4.0.5H2O (G) at 2θ values near 21.2°, 23.2°, 29.2° (Fig. S.7.4.iii; U.S. Geological Survey 2016). This is expected due to the high sulfate content in sulfuric acid. This explains the change in appearance of the T5 when investigated through stereo microscope and the possible reason for the change in AIV.

3.5.2 SEM and EDS of BDM After Immersion in Acids

The images obtained from SEM and the elemental compositions obtained from EDS analysis for soil + BDM immersed for 7 days are discussed in this section. Each of the scanned areas is approximately 120 μm by 120 μm square. All the SEM–EDS analysis results are presented in supplementary data (Fig. S.8.1–S.8.15) and (Table S.6.1–S.6.15).

SEM and EDS for soil + T1 showed the presence of Al, Si, Ca and Fe after immersion in nitric acid [Table S.6.1]. The elements Al, Si, Ca and Fe [Table S.6.2] are observed and present in soil + T1 after immersion in sulfuric acid. The elemental composition for soil + T1 after immersion in hydrochloric acid showed the presence of Al, Si, Ca and Fe and in addition to these, element Cl is also present [Table S.6.3]. It is observed that there is significant change in elemental analysis but is not highly deviating that of from virgin soil + T1 BDM. The increase in Fe content is solely due to the soil.

The elemental composition for soil + T2 after immersion in nitric acid revealed the presence of Al, Si and Fe [Table S.6.4]. EDS elemental analysis for soil + T2 after sulfuric acid the elements Al, Si, Ca and Fe [Table S.6.5] are present as seen in virgin soil + T2. Elemental composition for soil + T2 after immersion in hydrochloric acid showed the presence of Cl in addition to Al, Si, Ca and Fe [Table S.6.6]. The change in proportions of elements is observed from the results.

EDS analysis for soil + T3 is showed the presence of Al, Si, Ca and Fe when immersed in nitric acid (Table S.6.7). The presence of Cl is observed from elemental analysis of soil + T3 after immersed in hydrochloric acid in addition to presence of Al, Si, Ca and Fe (Table S.6.8). The elemental analysis for soil + T3 after immersion in sulfuric acid showed the presence of Al, Si, Ca and Fe (Table S.6.9) and are in comply with that of virgin soil + T3.

Elemental compositions for soil + T4 after immersion in nitric acid showed the presence of Al, Si and Fe (Table S.6.10). When T4 immersed in sulfuric acid, soil + T4 showed the presence of Al, Si, Ca and Fe. High rise in Fe content is observed when it immersed in sulfuric acid (Table S.6.11). Similarly, relative elemental composition for soil + T4 after hydrochloric acid attack revealed the presence Cl in addition to Al, Si, Ca and Fe (Table S.6.12). These elemental compositions results are in compliance with that virgin soil + T4.

After immersion of T5 in nitric acid, the elemental composition for soil + T5 displayed the presence of Al, Si, Ca and Fe (Table S.6.13). After hydrochloric acid attack the soil + T5 showed the presence of Cl in addition to Al, Si, Ca and Fe (Table S.6.14). The quantitative proportion for elements for soil + T5 after immersion in sulfuric acid showed the presence of to Al, Si, Ca and Fe (Table S.6.15). These results are in comply with that of virgin soil + T5.

3.5.3 Stereo Microscopy on BDM After Immersion in Acids

Figure 8 presents the stereo microscopic images for T1 particles after 7 days' immersion in each solution sulfuric acid, hydrochloric acid and nitric acid at 2.5× magnification. The dimensions of this image are identical to Fig. 4. Visual comparison of T1 before exposure to hydrochloric acid solution (5% v/v) shows whitish deposition on the surface (Fig. 8i). These deposits could be precipitation of chloride salts on the T1 surface. In case of nitric acid immersion, visual comparison of T1 before exposure to nitric acid solution (5% v/v) shows brownish white deposition on the surface (Fig. 8ii). These deposits may be precipitation of nitrate salts on the T1 surface. Immersion in sulfuric acid solution (5% v/v) shows yellowish white to brown deposition on the surface (Fig. 8iii). These deposits may be precipitation of sulfate salts on the T1surface. The stereo microscope images for remaining all types of BDM are presented in supplementary data (Fig. S.9.1–S.9.4). Immersion for 7 leads to formation of these salts on the surface of the BDM. Each of these depositions distorts the physical appearance of the CBDM and also reduces its impact value.

3.5.4 Aggregate Impact Value (AIV) for BDM After Immersion in Acids

The average AIV results (from three tests) of BDM specimens after immersion in different acids for 7 days are presented in Table S.7 in supplementary data. The results indicate that BDM is susceptible to the presence of acids. It is evident that the change in values of AIV is due to formation of salts on the surface of the BDM which can be confirmed by stereomicroscopy (Fig. 8). Sulfuric acid, nitric acid
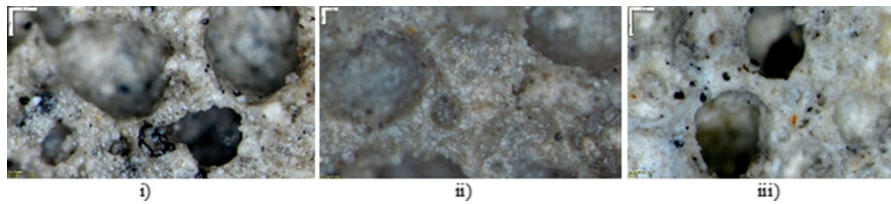
Fig. 8 Stereo microscopic image at 3.2 × magnification for T1 BDM particle after 7 day immersion in **i** hydrochloric acid (5% v/v) solution, **ii** nitric acid (5% v/v) solution, and **iii** sulfuric acid (5%v/v) solution

and hydrochloric acid immersions did not affect much of its AIV for T2, T3, T4 and T5 compared to before the immersion. But as the limiting value is 35%, the use of T1 (83.87% compared to 78.54% before the immersion) in hydrochloric acid and in the presence of chlorides are discouraged. The impact value for T1 is very less (39.05% and 23.91% compared to 78.54% before the immersion) in case of sulfuric acid, nitric acid immersion. It is highly noticeable and provides further confirmation on the better performance of T1. It observed for all types BDM that the presence of aggressive environment affected the AI value. Hence, proper care and observation is needed when it goes for practical applications.

3.5.5 Grain Size Analysis of BDM After Immersion in Acids for 7 Days

Gradation analysis is carried out for soil + chemically treated BDM blends in three kinds of acids as mentioned earlier. This is done to identify the effect of the acids on the grain size distribution of the BDM. Gradation analysis is conducted for T1 after immersion in the different acids is presented in this section (Fig. 9) and the values of C_u and C_c of T1 after immersion in these acids are presented in Table 7. Similarly, the gradation curves for T2, T3, T4 and T5 are presented in supplementary data (Fig. S.10.1–S.10.4). After exposure to these acids, BDM has got salts deposited on its surface, leading to significant changes in gradation curves. Results show that T1 is highly affected by chemical environment for 7 days. The different acids have significant effect on the values of C_u and there is a drastic decrease in the value of C_c for T1 after exposure to different acids and the highest effect is observed for sulfuric acid. Remaining types of BDM has got changes in curves as well as in values of shape factors C_u and C_c presented in supplementary data (Table S.7.1–S.7.4). These acids

affected the structure of the BDM particles as shown in stereo microscope images, hence affected the shape characteristics for BDM. It clearly indicates that proper care should be taken while using BDM in chemically contaminated areas.

3.5.6 Specific Gravity and Water Absorption for BDM After Immersion in Acids

The results of the specific gravity for BDM specimens after immersion in different acids 7 days are tabulated in supplementary data table S.8.1. Sulfuric acid, hydrochloric acid and nitric acid immersions highly affected the specific gravity values (1.06, 1.32 and 1.05 compared to 1.33 before the immersion). SG values for other types of BDM are deviated from that of virgin BDM (Table S.8.1). It concludes that the presence of chemical environment in field conditions, will shows its effect on the performance of the BDM as it is clearly visible from the results.

The water absorption results for BDM after immersion in different acids 7 days are presented in supplementary data (Table S.8.2). The different chemicals have significant effect on the values of water absorption for T2, T3 and T5 and are deviating from that of Virgin BDM. However, there is significant increase in water absorption values for T1 and T4 clearly indicating that when these BDM undergo chemical reaction, will affect the performance of BDM. The proper care should be taken to use these BDM in such aggressive environmental conditions.

3.5.7 Effect of Acids on Angle of Internal Friction of BDM

Large shear box test is conducted to find out the angle of internal friction of soil-BDM mix after immersion in the various aforementioned acids. The large shear box tests show that the maximum values of friction
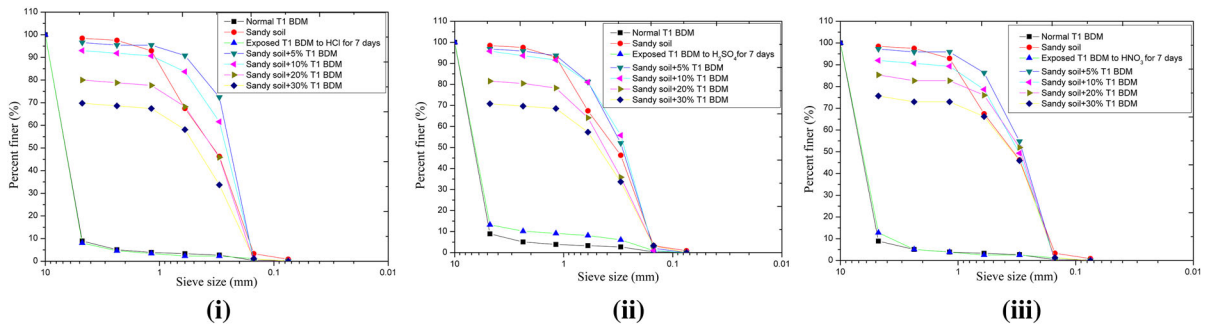
Fig. 9 Grain size analysis for T1 immersed for 7 days in, **i** hydrochloric acid, **ii** sulfuric acid and **iii** nitric acid

Table 7 Values of shape factors of soil at different proportions of T1 immersed in different acids

Acids used Proportion of BDM in soil	T1 immersed in HNO_3		T1 immersed in HCl		T1 immersed in H_2SO_4	
Soil + T1	C_u	C_c	C_u	C_c	C_u	C_c
Soil	2.5	0.9	2.5	0.9	2.5	0.9
T1 before immersion	1.45	0.95	1.45	0.95	1.45	0.95
T1 immersed	1.79	1.10	1.44	0.94	2.5	1.54
5% T1	1.76	1.03	1.35	0.93	1.76	0.86
10% T1	2.23	0.81	1.52	0.9	1.88	0.76
20% T1	2.21	0.82	2.44	0.67	2.77	0.69
30% T1	2.64	0.69	3.42	0.63	3.51	0.54

angle (φ) is achieved when the cohesionless soil is mixed with approximately in the range of 17–23% of BDM by weight. Thus this test is conducted at 20% of replacement of soil with immersed BDM. The results, tabulated in Table S.9 in supplementary data, indicates that when the optimum BDM content added to the soil is exposed to such acids, the friction angle significantly varies from that of the virgin BDM. The friction angle (φ) of T3, immersed in acid for 7 days, decreases with respect to virgin T3. For remaining types of BDM, internal friction angle (φ) is in compliance with that of virgin BDM. Hence, proper measures must be adopted while using BDM as a foreign additive in soil in such practical scenarios.

4 Conclusion

The construction and demolition waste (CDW) generation are in focus in the present world to achieve sustainability. Recycle and reuse of these materials serve double benefit of, reducing the costs associated

with the disposal process, and at the same time helping the environment by avoiding waste disposal into dumping yards. It is observed that the primary components of CDW are building derived materials (BDM). The present study thus adopts a novel technique to reuse BDM and blend them with soil in different proportions (0–30%) to improve their strength properties. Additionally, the reuse of BDM will also reduce the need for production of fresh aggregates for soil replacement, thereby preserving natural limestone content and reducing the amount of CO_2 emissions associated with their production and processing. Further studies are required to improve its characteristics when BDM is exposed to such acids in real-life ground improvement applications. The important findings of the present study can be summarized as follows:

- The mineralogical and microanalysis results confirm the presence of crystalline phases in different types of BDM. From EDS analysis, the change in proportions of elements is observed after immersion. These results further show that the BDM are

highly influenced in the presence of acids. Sulfuric acid had the most significant deterioration on the performance of the BDM.

- The particle size distribution curve of crushed lightweight concrete indicates that the gravel, soil and silt and clay sized particles present are 91.08, 8.63 and 0.29% respectively. Thus the BDM can be classified as a heavyweight material. Similarly, crushed marble tiles, crushed high strength concrete, crushed normal Portland cement concrete, and crushed bricks are also reported as heavy weight materials. Also the values of the shape parameters of poorly graded cohesion less soil improved significantly when mixed with BDM. Meanwhile, the values of C_u and C_c for soil mixed with different types of BDM are highly affected in presence of acids, the maximum effect being that of sulfuric acid.

- The addition of all types BDM to soil significantly increased the internal angle friction (φ) of soil. The average optimum percentage of all types of BDM to be added in soil was found to be in the range of 17–23%.

- The internal angle of friction for crushed high strength concrete is highly affected by the acids and it is observed that the internal angle of friction of crushed lightweight concrete, crushed marble tiles, crushed normal Portland cement concrete, and crushed bricks decreases the acids tend to corrode the BDM and make it more angular.

- The formation of deposits on the surface of BDM due to presence of dissolved salts in various acids creates distortion in the physical appearance of the BDM when observed through the stereomicroscope.

- The AIV for crushed lightweight concrete is high (79%) and is less durable, whereas crushed marble tiles, crushed high strength concrete, crushed normal portland cement concrete, and crushed bricks showed high resistance and durable can be used as partial replacement in soil. The acids caused significant effect on the AI value of crushed lightweight concrete. Similarly, it is noticed the effect of acids in AI values of crushed marble tiles, crushed high strength concrete, crushed normal portland cement concrete, and crushed bricks. The results suggest that the durability of BDM in such aggressive chemical environment is significantly varying and needs proper care in real life applications. The advantages of reusing BDM for practical purposes are the prevention of dumping them as solid waste and also promoting an economic technique to enhance the compaction characteristics of soil. Thus, further studies are required to improve the durability characteristics of BDM if they are to be used as an inclusion material in soils containing such chemical contaminant.

References

Arulrajah A, Piratheepan J, Aatheesan T, Bo MW (2011) Geotechnical properties of recycled crushed brick in pavement applications. J Mater Civ Eng 23(10):1444–1542. https://doi.org/10.1061/(ASCE)MT.1943-5533.0000319

Arulrajah A, Piratheepan J, Ali YMM, Bo MW (2012) Geotechnical properties of recycled concrete aggregate in pavement sub-base applications. Geotech Test J 35(5):1–9

ASTM C131/C131M-14 (2006) Standard test method for resistance to degradation of small-size coarse aggregate by abrasion and impact in the Los Angeles machine. ASTM International, West Conshohocken

ASTM D3080/D3080M-11 (2011) Standard test method for direct shear test of soils under consolidated drained conditions. ASTM International, West Conshohocken

ASTM D6913/D6913M-17 (2017) Standard test methods for particle-size distribution (gradation) of soils using sieve analysis. ASTM International, West Conshohocken

ASTM D854-06e1 (2016) Standard test methods for specific gravity of soil solids by water pycnometer. ASTM International, West Conshohocken

ASTM C127-15 (2016) Standard test method for relative density (specific gravity) and absorption of coarse aggregate. ASTM International, West Conshohocken

Bhattacharyya SK, Minocha AK, Garg M, Singh J, Jain N, Maiti S, Singh SK (2013) GAP0072 (DST Project), demolition wastes as raw materials for sustainable construction products. CSIR-CBRI News Lett 33(2):1–2

Bontempi E, Zacco A, Borgese L, Gianoncelli A, Ardesi R, Deper LE (2010) A new method for municipal solid waste incinerator (MSWI) fly ash inertization, based on colloidal silica. J Environ Monit 12:2093–2099

Cardoso EJBN, Vasconcellos RLF, Bini D, Miyauchi MYH, Santos CA, Alves PRL, Paula AM, Nakatani AS, Pereira

JM, Nogueira MA (2013) Soil health: looking for suitable indicators. What should be considered to assess the effects of use and management on soil health? Sci Agric 70:89–274. https://doi.org/10.1590/s0103-90162013000400009

Christopher AB, Craig HB, Tuncer BE (2008) Comparison of shear strength of soil backfills measured in small-scale and large scale direct shear tests. Can Geotech J 45:1224–1236

Courard L, Michel F, Delhez P (2010) Use of concrete road recycled aggregates for roller compacted concrete. Constr Build Mater 24(3):390–395. https://doi.org/10.1016/j.conbuildmat.2009.08.040

Debieb F, Kenai S (2008) The use of coarse and fine crushed bricks as aggregate in concrete. J Constr Build Mater 22(5):886–893

Edil TB (2015) Sustainable geotechnical applications: Tire derived aggregate in geotechnical and environmental applications - part V of VI (AWI062811): webinar hosted by ASCE GeoInstitute and Continuing Education, 2015

EI Gohary MA, AI Naddaf MM (2009) Characterization of bricks used in the external casing of roman bath walls, Gadara-Jordan. Mediterr Archaeol Archaeom 9(2):29–46

Fang S, Zhang K, Zhang H, Zhang B (2015) A study of traditional blood lime mortar for restoration of ancient buildings. Cem Concr Res 76:232–241

Harmon K (2014) Engineering properties of structural lightweight concrete. http://www.stalite.com/uploads/EngineeringProperties.pdf. Accessed 23 May 17

Hasan U, Chegenizadeh A, Budihardjo MA, Nikraz H (2016) Experimental evaluation of construction waste and ground granulated blast furnace slag as alternative soil stabilizers. J Geotech Geol Eng 34(6):1–16

Hoyos LR, Puppala AJ, Ordonez CA (2011) Characterization of cement fiber-treated reclaimed asphalt pavement aggregates: preliminary investigation. J Mater Civ Eng 23(7):977–989. https://doi.org/10.1061/(ASCE)MT.19435533.0000267

IS 2386-3 (2011a) Methods of test for aggregates for concrete, part 3: specific gravity and water absorption. Bureau of Indian Standards, New Delhi

IS 2386-Part 4 (2011b) Methods of test for aggregates for concrete, part 4: mechanical properties. Bureau of Indian Standards, New Delhi

IS 2720-Part 39 (1979) Method of test for soils: direct shear test for soils containing gravel. Bureau of Indian Standards (BIS), New Delhi. Reaffirmed 2002

IS: 2720-Part 4 (1985) Methods of test for soils, part 4: grain size analysis. Bureau of Indian Standards (BIS), New Delhi

Kar A, Ray I, Halabe UB, Unnikrishnan A, Dawson AB (2014) Characterizations and estimation of alkali activated binder paste from microstructures. Int J Concr Struct Mater 8(3):213–228

Kupwade PK, Allouche E (2011) Effect of alkali silica reaction (ASR) in geopolymer concrete. In: World of Coal Ash (WOCA) conference, Denver, CO, USA

Lee JH, Salgado R, Bernal A, Lovell CW (1999) Shredded tires and rubber–soil as light weight backfill. J Geotech Geoenviron Eng ASCE 125(2):132–141

Lim M, Han GC, Ahn JW, You KS (2010) Environmental remediation and conversion of carbon dioxide (CO$_2$) into useful green products by accelerated carbonation technology. Int J Environ Res Public Health 7(1):203–228

McKelvey D, Sivakumar V, Bell A, McLaverty G (2002) Shear strength of recycled construction materials intended for use in vibro ground improvement. Proc Inst Civ Eng UK 6(2):59–68

Melton JS (2015) Recycled base aggregates in pavement applications—part III of VI (AWI051611). Sustainable geotechnical applications: webinar hosted by ASCE

Meyer C (2004) Concrete materials and sustainable development in the United States. Structual Engineering International, Zurich, IABSE, 14/3 August, pp 203–207

Mindess S, Young JF, Darwin D (2003) Concrete. Prentice Hall, Pearson Education Inc, New Jersey

Misapor (2014) Technical data international. http://www.archiproducts.com/en/products/13344/foam-glass-gravel-misapor-misapor.html. Accessed 23 May 17

Poon CS, Chan D (2006) Feasible use of recycled concrete aggregates and crushed clay brick as unbound road subbase. Constr Build Mater 20:578–585

Rahman MA, Arulrajah A, Piratheepan J, Bo MW, Imteaz MA (2014a) Resilient modulus and permanent deformation responses of geogrid-reinforced construction and demolition materials. J Mater Civ Eng 26:512–519

Rahman MA, Imteaz M, Arulrajah A, Disfani MM (2014b) Suitability of recycled construction and demolition aggregates as alternative pipe backfilling materials. J Clean Prod 66:75–84

Rao A, Jha KN, Misra S (2007) Use of aggregates from recycled construction and demolition waste in concrete. Resour Conserv Recycl 50(1):71–81

Rathje E, Trejo D, Folliard K (2006) Use of recycled asphalt pavement and crushed concrete as backfill for mechanically stabilized earth retaining walls. Research report 0-4177-S. Center for Transportation Research, The University of Texas at Austin, Austin

Sadrekarimi A, Olson SM (2009) Shear band formation observed in ring shear tests on soils. J Geotech Geoenviron Eng 136(2):366–375

Sobhan K, Krizek RJ (1998) Resilient properties and fatigue damage in stabilized recycled aggregate base course material. Transp Res Rec 1611(1):28–37. https://doi.org/10.3141/1611-04

Suluguru AK, Jayatheja M, Kar A, GuhaRay A, Surana SR, James N (2017) Experimental studies on the microstructural, physical and chemical characteristics of building derived materials to assess their suitability in ground improvement. Constr Build Mater 156:921–932

Victorian Recycling Industries, Annual Survey (2004–2005), pp 1–28, Sustainability Victoria, Melbourne, Australia

Taha R, Al-Harthy A, Al-Shamsi K, Al-Zubeidi M (2002) Cement stabilization of reclaimed asphalt pavement aggregate for road bases and subbases. J Mater Civ Eng 14(3):239–245. https://doi.org/10.1061/(ASCE)0899-1561(2002)14:3(239)

Tam VWY, Tam CM (2007) Crushed aggregates production from centralized combined and individual waste sources in Hong Kong. Constr Build Mater 21(4):879–886. https://doi.org/10.1016/j.conbuildmat.2005.12.016

Taylor HFW (1997) Cement chemistry, 2nd edn. Thomas Telford, London

The Hindu, Construction waste recycling plants soon (2017) http://www.thehindu.com/todays-paper/tp-national/tp-telangana/work-on-recycling-plants-to-start-soon/article20007457.ece; Accessed 09 Nov 2017

USEPA (2017) Lifecycle challenge competition seeks new ideas to reduce construction and demolition debris, 2015. http://www3.epa.gov/region9/waste/solid/construction/. Accessed 02 Feb 2017

U. S. Geological Survey Open-File Report 01-041 (2016) A laboratory manual for X-ray powder diffraction. http://pubs.usgs.gov/of/2001/of01-041/htmldocs/links.htm

Yildirim M, Kipcak AS, Senberber FT, Asensio MO, Derun EM, Piskin S (2015) The determination of the potassium nitrate, sodium hydroxide and boric acid molar ratio in the synthesis of potassium borates via hydrothermal method. World Acad Sci Eng Technol Int J Chem Mol Nucl Mater Metall Eng 9(5):597–600

Zuquan J, Wei S, Yunsheng Z, Jinyang J, Jianzhong L (2007) Interaction between sulfate and chloride solution attack of concretes with and without fly ash. Cem Concr Res 37(8):1223–1232